Open Archive TOULOUSE Archive Ouverte (OATAO)

OATAO is an open access repository that collects the work of Toulouse researchers and makes it freely available over the web where possible.

Whole-exome sequencing in osteosarcoma reveals important heterogeneity of genetic alterations

M. Bousquet[1], C. Noirot[2], F. Accadbled[3], J. Sales de Gauzy[3], M. P. Castex[4], P. Brousset[1,5]*
& A. Gomez-Brouchet[5,6]

[1]Cancer Research Center of Toulouse, INSERM U1037, laboratoire d'excellence Labex TOUCAN, Toulouse; [2]Genotoul Bioinfo, INRA, Castanet Tolosan; Departments of [3]Pediatric Orthopedics; [4]Pediatric Oncology, Hôpital des enfants, Toulouse; [5]Department of Pathology, IUCT-Oncopole, CHU de Toulouse and Toulouse University, Toulouse; [6]Pharmacology and Structural Biology Institute, CNRS UMR5089, Toulouse, France

Background: Whole-genome sequencing studies have recently shown that osteosarcomas (OSs) display high rates of structural variation, i.e. they contain many somatic mutations and copy number alterations. *TP53* and *RB1* show recurrent somatic alterations in concordant studies, suggesting that they could be key players in bone oncogenesis.

Patients and methods: we carried out whole-genome sequencing of DNA from seven high-grade OS samples matched with normal tissue from the same patients.

Results: We confirmed the presence of genetic alterations of the *TP53* (including novel unreported mutations) and *RB1* genes. Most interestingly, we identified a total of 84 point mutations and 4 deletions related to 82 different genes in OS

samples, of which only 15 have been previously reported. Interestingly, the number of mutated genes (ranging from 4 to 8) was lower in *TP53mut* cases compared with *TP53wt* cases (ranging from 14 to 45). This was also true for the mutated *RB1* case. We also observed that a dedifferentiated OS harboring *MDM2* amplification did not carry any other mutations.

Conclusion: This study suggests that bone oncogenesis driven by *TP53* or *RB1* mutations occurs on a background of relative genetic stability and that the dedifferentiated OS subtype represents a clinico-pathological entity with distinct oncogenic mechanisms and thus requires different therapeutic management.

introduction

Osteosarcoma (OS) is the most common primary malignant type of bone cancer and has a worldwide incidence of approximately one to three cases per million annual, with a higher incidence in adolescents (0.8–1.1/100 000/year for ages 15–19). The 2013 World Health organization (WHO) classification distinguishes different OS subtypes on the basis of both their location in relation to the bone cortex (central or surface OS) and their grade (low, high or intermediate [1]. High-grade OS are themselves divided into different subtypes: conventional (the most common one, 90% of all OS), telangiectasic and small-cell OS (respectively 4% and 1.5% of all OS) and the dedifferentiated OS [1]. This latter corresponds to the transformation of a low-grade OS into an OS of higher grade. Low-grade and its dedifferentiated form are defined by a simple genomic profile with episomal ring neochromosomes containing high-level amplification of *MDM2* (murine double-minute type 2) and *CDK4* (cyclin-dependent kinase 4) [2, 3]. Microscopically, low-grade OS is characterized by a paucicellular stroma of fusiform cells harboring minor cytonuclear atypia and well-differentiated bone trabeculae [1]. Dedifferentiated OS is most often composed of cells with larger atypia and mitosis than its low-grade counterparts and by the presence of an immature osteoid production. Tumor necrosis may also be present [1, 3]. In the dedifferentiated form, areas of low- and high-grade tumor may or may not coexist. When the low- grade contingent is not present on biopsy specimens or surgical resection, dedifferentiated OS could be misdiagnosed with conventional OS. The diagnosis of the dedifferentiated form is made on the molecular signature (amplification of *MDM2* gene) [3]. Conversely, the other high-grade OS are complex genomic sarcomas with multiple numerical and structural chromosomal aberrations that present no specific diagnostic signature [1].

Several heritable genetic syndromes predispose to OS: Li–Fraumeni syndrome or heritable retinoblastomas are related to germ-line mutations in the *TP53* and *RB1* tumor suppressor genes, respectively [4, 5]. The genetic instability of OS results in recurrent amplification and DNA copy number gains at distinct chromosomal regions [1]. Recently, whole-genome sequencing studies have shown that among pediatric cancers, OS have the highest rate of structural variation, i.e. they contain many somatic mutations and copy number alterations [6, 7]. A few recurrent single-nucleotide variations or recurrent point mutations have been found [7]. These studies have confirmed the major roles of recurrent alterations of the *TP53* and *RB1* genes in OS (80%–90% and 10%–39%, respectively). The majority of *TP53* mutations are rearrangements with breakpoints confined to the first intron of the gene [7, 8]. This is therefore a particularly unstable region that is sensitive to structural variations that occur before inactivation of *TP53* and that are likely to be the initiating factors in OS development [7]. Another recent study has also confirmed the importance and prevalence of *TP53* and *RB1* inactivation by genomic events, which either affect the *TP53* or *RB1* genes directly or alter *TP53/RB1*-interacting genes. In this study, the authors also reported that 75% of somatic events lead to the direct or indirect inactivation of *TP53* [6]. Besides *TP53* and *RB1*, the *ATRX*, *DLG2*, *RUNX2* and *PTEN* genes have been shown to incur recurrent somatic alterations in 30%, 30%, 52%, 18–55% and 44% of OS, respectively [7]. The *ATRX* gene is known to regulate telomere maintenance and could therefore have an important role in OS development [9]. Alterations in *CDC27*, a gene controlling the cell cycle, and the *MUC4* and *EI24* genes known to encode tumor suppressors, were also recently reported [10]. In addition, genome sequencing data have shown that the novel genetic mechanism referred to as chromothripsis (Greek; chromos for chromosome, thripsis for shattered into pieces) is involved in 33% of primary OS compared with 2%–3% of cancers overall [11]. Chromothripsis appears to be a cataclysmic event in which a single or in some cases, a few chromosomes are broken into many pieces and then stitched back together [11, 12]. Chromothripsis may lead to the generation of amplifications of one or more genes or to the deletion of one or more tumor suppressor genes. It may also explain the sudden onset of OSs and the complexity and heterogeneity of the OS genome [1, 11, 12]. In a recent study, exome profiles in one patient showed almost 3000 somatic single-nucleotide variants (SNVs) and small indels and more than 2000 copy number variants in different chromosomes, reinforcing the major role of this phenomenon [10]. Kataegis (a pattern of localized hypermutation in a SNV) has also been reported in OS, although the study of Perry et al. [6] reported a higher prevalence (85% of OS) than that reported by Chen et al. [7] (50% of OS). However, this process is certainly less important because it does not occur in the most recurrently mutated genes [7].

To further refine the landscape of somatic mutations in pediatric OS, we carried out exome sequencing of DNA from seven OS samples matched with normal tissues from the same patients (Table 1). Three important findings arise from this work. Our results confirm: (i) the heterogeneity of genetic alterations in conventional high-grade OS by providing new unreported mutations, (ii) the dominant role of *TP53* and *RB1* gene inactivation in the development of OS, and (iii) that dedifferentiated OS is a separate entity with a different pathophysiology from that of conventional high-grade OS.

Table 1. Mutated genes detected by whole-exome sequencing

Patient	Gene	Chr	Position	REF	ALT	dbSNP	Effect	Type
1	TP53[a]	chr17	7 578 275	G	A	None	STOP_GAINED	Mut
1	PSD4[a]	chr2	113 942 572	T	G	None	NON_SYNONYMOUS_CODING	Mut
1	CLNS1A	chr11	77 333 719	C	A	None	SPLICE_SITE_ACCEPTOR	Mut
1	SPTB	chr14	65 253 678	C	T	None	NON_SYNONYMOUS_CODING	Mut
1	TSC2[a]	chr16	2 138 087	G	A	None	NON_SYNONYMOUS_CODING	Mut
1	CHL1	chr3	425 527	G	T	None	NON_SYNONYMOUS_CODING	Mut
2	RB1[a]	chr13	49 039 501	C	A	None	STOP_GAINED	Mut
2	GPRC6A[a]	chr6	117 121 780	A	T	None	NON_SYNONYMOUS_CODING	Mut
2	C1orf174	chr1	3 807 588	T	G	None	NON_SYNONYMOUS_CODING	Mut
2	LTF	chr3	46 506 382	C	T	None	UTR_5_PRIME	Mut
2	POLD2	chr7	44 154 485	C	T	None	NON_SYNONYMOUS_CODING	Mut
2	CXorf22	chrX	35 969 379	G	C	None	NON_SYNONYMOUS_CODING	Mut
3	TP53[a]	chr17	7 578 455	C	A	None	NON_SYNONYMOUS_CODING	Mut
3	TP53[a]	chr17	7 578 451	ATGG	A	None	CODON_CHANGE_PLUS_CODON_DELETION	Indel
3	TP53[a]	chr17	7 578 434	ACTGCTTGTAGATGG	A	None	FRAME_SHIFT	Indel
3	ABCA13[a]	chr7	48 452 019	C	A	None	NON_SYNONYMOUS_CODING	Mut
3	RP1L1[a]	chr8	10 466 225	C	G	None	NON_SYNONYMOUS_CODING	Mut
3	OR8I2	chr11	55 861 061	C	T	None	NON_SYNONYMOUS_CODING	Mut
3	CACNA1C	chr12	2 229 523	T	C	None	NON_SYNONYMOUS_CODING	Mut
3	STYK1	chr12	10 787 262	A	C	None	UTR_5_PRIME	Mut
3	WFDC9	chr20	44 236 751	A	G	None	STOP_LOST	Mut
3	NOBOX	chr7	144 094 557	G	A	None	NON_SYNONYMOUS_CODING	Mut
3	PIWIL2	chr8	22 137 017	G	A	None	NON_SYNONYMOUS_CODING	Mut
5	CR1[a]	chr1	207 751 260	A	G	rs202070239	NON_SYNONYMOUS_CODING	Mut
5	CR1[a]	chr1	207 751 252	T	C	rs200111726	NON_SYNONYMOUS_CODING	Mut
5	LRRC16B[a]	chr14	24 537 870	A	C	None	NON_SYNONYMOUS_CODING	Mut
5	SYNE2[a]	chr14	64 688 390	C	T	rs35700578	NON_SYNONYMOUS_CODING	Mut
5	SALL1[a]	chr16	51 175 831	G	A	None	NON_SYNONYMOUS_CODING	Mut
5	DNAH6[a]	chr2	84 848 403	G	A	rs185981876	NON_SYNONYMOUS_CODING	Mut
5	ADAMTS16[a]	chr5	5 319 934	A	G	rs58353460	UTR_3_PRIME	Mut
5	C1orf189	chr1	154 178 828	CTCT	C	None	UTR_5_PRIME	Indel
5	EPS8L3	chr1	110 292 938	CG	C	rs148530481	UTR_3_PRIME	Indel
5	NAV2	chr11	20 075 708	A	G	None	NON_SYNONYMOUS_CODING	Mut
5	TENM4	chr11	78 381 189	C	A	None	NON_SYNONYMOUS_CODING	Mut
5	KRT72	chr12	52 984 733	G	C	rs34769047	NON_SYNONYMOUS_CODING	Mut
5	KRT80	chr12	52 574 730	G	A	rs141379526	NON_SYNONYMOUS_CODING	Mut
5	ARHGAP5	chr14	32 561 778	C	T	rs115598823	NON_SYNONYMOUS_CODING	Mut
5	COQ6	chr14	74 428 000	A	T	rs2074930	NON_SYNONYMOUS_CODING	Mut
5	DCAF5	chr14	69 521 338	C	A	rs116182003	NON_SYNONYMOUS_CODING	Mut
5	G2E3	chr14	31 067 748	G	A	rs17096934	NON_SYNONYMOUS_CODING	Mut
5	GZMH	chr14	25 075 810	T	A	rs115493987	STOP_LOST	Mut
5	MLH3	chr14	75 514 200	T	C	rs28756988	NON_SYNONYMOUS_CODING	Mut
5	PAPLN	chr14	73 721 300	C	T	rs17126354	NON_SYNONYMOUS_CODING	Mut
5	PLEKHH1	chr14	68 042 573	C	A	rs186582399	NON_SYNONYMOUS_CODING	Mut
5	RBM23	chr14	23 374 568	C	T	rs34246954	NON_SYNONYMOUS_CODING	Mut

5	RNASE10	chr14	20 978 738	G		T	rs74037153	NON_SYNONYMOUS_CODING	Mut
5	RNASE13	chr14	21 501 843	G		A	rs116165621	UTR_3_PRIME	Mut
5	TSHR	chr14	81 422 169	A		G	rs147137913	NON_SYNONYMOUS_CODING	Mut
5	COQ9	chr16	57 493 629	G		C	rs61730662	NON_SYNONYMOUS_CODING	Mut
5	GP2	chr16	20 330 955	G		T	None	NON_SYNONYMOUS_CODING	Mut
5	NUBP2	chr16	1 838 050	A		G	rs57822546	NON_SYNONYMOUS_CODING	Mut
5	CHST8	chr19	34 263 855	G		A	None	NON_SYNONYMOUS_CODING	Mut
5	DHDH	chr19	49 436 982	G		C	rs10401800	NON_SYNONYMOUS_CODING	Mut
5	TMEM221	chr19	17 556 074	C		T	None	NON_SYNONYMOUS_CODING	Mut
5	PLB1	chr2	28 849 317	G		A	None	STOP_GAINED	Mut
5	SH3YL1	chr2	231 067	G		C	None	NON_SYNONYMOUS_CODING	Mut
5	SCP2D1	chr20	18 794 656	T		A	None	NON_SYNONYMOUS_CODING	Mut
5	MIRLET7BHG	chr22	46 505 806	C		G	rs12159905	EXON	Mut
5	PKDREJ	chr22	46 656 242	A		G	rs34798212	NON_SYNONYMOUS_CODING	Mut
5	TMPRSS6	chr22	37 464 655	C		G	rs80252000	SPLICE_SITE_DONOR	Mut
5	ATR	chr3	142 272 671	T		C	None	NON_SYNONYMOUS_CODING	Mut
5	MANBA	chr4	103 579 032	G		A	rs370002189	NON_SYNONYMOUS_CODING	Mut
5	MIR6082	chr4	172 107 395	C		T	rs28570267	EXON	Mut
5	CEP120	chr5	122 714 044	T		C	rs61744334	NON_SYNONYMOUS_CODING	Mut
5	TRDN	chr6	123 714 778	C		T	rs35047281	NON_SYNONYMOUS_CODING	Mut
5	CTNNAL1	chr9	111 735 031	G		C	rs16913734	NON_SYNONYMOUS_CODING	Mut
5	GLDC	chr9	6 606 634	C		T	rs28617412	NON_SYNONYMOUS_CODING	Mut
5	ESX1	chrX	103 495 445	G		C	None	NON_SYNONYMOUS_CODING	Mut
6	DUSP27[a]	chr1	167 096 814	G		T	None	NON_SYNONYMOUS_CODING	Mut
6	VPS13D[a]	chr1	12 336 850	G		C	None	NON_SYNONYMOUS_CODING	Mut
6	EFCAB6[a]	chr22	44 022 541	A		G	None	NON_SYNONYMOUS_CODING	Mut
6	GCSAML	chr1	247 726 894	A		G	None	NON_SYNONYMOUS_CODING	Mut
6	SYNC	chr1	33 161 551	C		G	None	NON_SYNONYMOUS_CODING	Mut
6	OR9Q1	chr11	57 947 475	T		G	None	NON_SYNONYMOUS_CODING	Mut
6	TRPC4	chr13	38 320 482	C		A	None	NON_SYNONYMOUS_CODING	Mut
6	PFAS	chr17	8 170 715	C		G	None	NON_SYNONYMOUS_CODING	Mut
6	CATSPERD	chr19	5 757 865	C		A	None	NON_SYNONYMOUS_CODING	Mut
6	DLL1	chr6	170 594 743	C		T	None	NON_SYNONYMOUS_CODING	Mut
6	DDHD2	chr8	38 109 710	C		G	None	NON_SYNONYMOUS_CODING	Mut
6	MCMDC2	chr8	67 808 447	A		C	None	NON_SYNONYMOUS_CODING	Mut
6	TAF1L	chr9	32 632 563	C		A	None	NON_SYNONYMOUS_CODING	Mut
6	NRK	chrX	105 189 927	A		C	None	NON_SYNONYMOUS_CODING	Mut
7	TP53[a]	chr17	7 577 018	C		T	None	SPLICE_SITE_DONOR	Mut
7	PLCB2	chr15	40 590 865	C		T	None	NON_SYNONYMOUS_CODING	Mut
7	HID1	chr17	72 956 123	C		T	None	NON_SYNONYMOUS_CODING	Mut
7	KLB	chr4	39 436 255	T		A	None	NON_SYNONYMOUS_CODING	Mut
7	GRIA1	chr5	153 181 955	G		A	None	NON_SYNONYMOUS_CODING	Mut

[a]In dark gray genes previously described in Perry et al. [6] and in light gray by Chen et al. [7].

patients and methods

OS samples and cell lines

Seven OS samples coming from initial biopsy and seven matched control DNA samples were collected from patients registered at the 'CRB cancer des Hôpitaux de Toulouse; BB-0033-00014' collection. This study had approval from institutional and national ethics committees. Thawed samples were obtained after informed consent in accordance with the Declaration of Helsinki and after authorization of the French ministry of higher education and research (declaration DC 2009-989; DC-2011-1388; transfer agreement AC-2008-820; AC-2011-130). Clinical and biological annotations were consistent with CNIL (Comité National Informatique et Libertés) guidelines. Samples were stored in the certified biobank of the Hôpitaux de Toulouse. Control samples corresponded to tissues taken from surgical resection that were obtained after chemotherapy treatment. The percentage of cancer cells remaining in control samples was evaluated by morphological analysis after decalcification and hematoxylin–eosin staining.

Six patients had high-grade conventional OS. Among them, five were good responders with a percentage of residual cells lower than 10% and are alive. One was a poor responder with 27% residual cells (patient 5). He died from lung metastases.

Patient 4 presented with intramedullary (central) dedifferentiated OS (Figure 1A–C) with MDM2 overexpression (Figure 1D) and amplification (confirmed by qPCR). Due to a dedifferentiated component in the diagnostic biopsy, he received neoadjuvant chemotherapy. He was a good responder according to the surgical resection analysis and he is still alive (supplementary Table S1, available at *Annals of Oncology* online).

Two osteoblastic cell lines (TF13 and TF15) were also used as controls [13]. DNA sample integrity was evaluated by agarose gel electrophoresis.

exome sequencing

Three micrograms of qualified genomic DNA were randomly fragmented by Covaris and then adapters were ligated to both ends of the resulting fragments (200–300 bp). Extracted DNA was amplified by ligation-mediated PCR (LM-PCR), then purified and hybridized to the Roche NimbleGen SeqCap EZ Exome probe. Nonhybridized fragments were washed out. Both noncaptured and captured LM-PCR products were subjected to quantitative PCR to estimate the magnitude of enrichment. Each captured library was then loaded on to a Hiseq2000 (Illumina) platform. High-throughput sequencing for each captured library was carried out independently to ensure that each sample met the desired average fold-coverage of 50×. Raw image files were processed by Illumina base calling Software 1.7 for base calling with default parameters and the sequences of each individual were generated as 91-bp paired-end reads.

bioinformatical analysis

First, the adapter sequences in the raw data, generated from the Illumina pipeline, were removed, and low-quality reads that had too many Ns or low base quality were discarded. This step produced the 'clean data'. Second, the Burrows-Wheeler Aligner [BWA mem (0.7.9a-r786)] was used to carry out the alignment against the human reference genome Hg19. Samples were then realigned and recalibrated with GATK (v3.0). HaplotypeCaller was used to call variants using standard options and a bed of exome region. The annotation was performed with SnpEff (v3.6c) against Hg19 with the option 'cancer'. For SNP and indels, we applied the following filters: the mutation must have not existed in cell line samples (even one read) and, for control patient samples, the mutation must have had a minimum allele frequency (MAF) below: 5% for control patient 1, 15% for control patient 2, 5% for control patient 3, 0% for control patient 4, 40% for control patient 5, 10% for control patient 6 and 10% for control patient 7. These percentages correspond to the putative contamination of remaining cancer cells. Only mutations with a depth higher than 20 were considered. Moreover, we selected mutations and indels in tumor samples with MAF >30% and MAF >20% respectively. Finally, for each mutation, the tumor sample MAF had to be 2.5 times higher than the MAF of the matched control sample and, for each
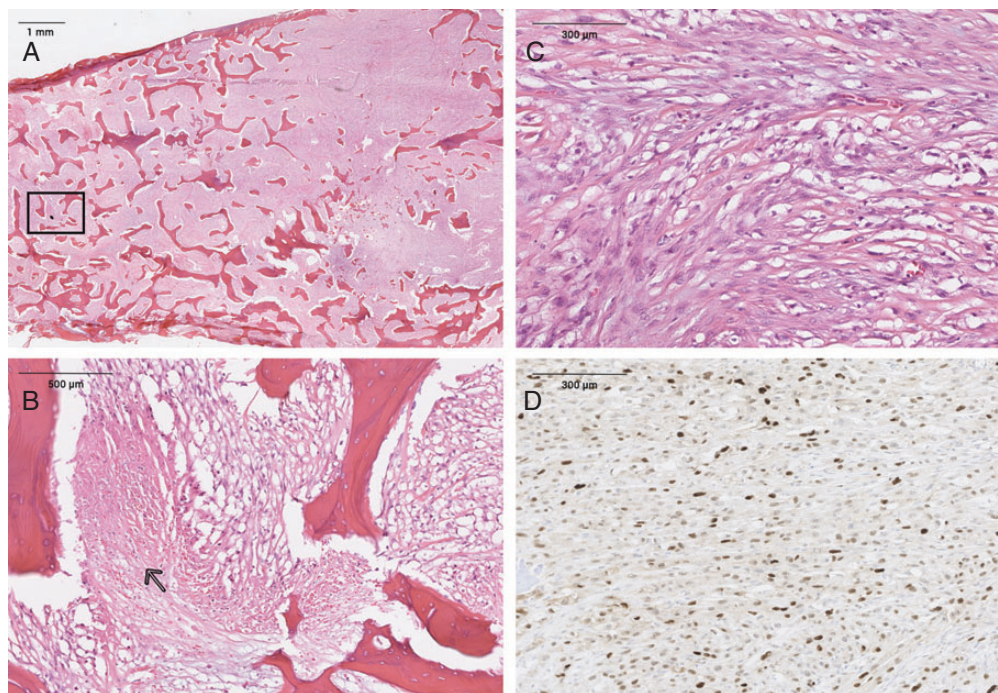

Figure 1. (A) Histological appearance of an intramedullary (central) dedifferentiated osteosarcoma (H&E). (B) Magnification of rectangle shown in A. Necrosis area (open arrow) in a dedifferentiated osteosarcoma and immature neoplastic osteoid (black arrow) (H&E). (C) Spindle cells with moderate nuclear atypia, mitosis and immature neoplastic osteoid production (H&E). (D) MDM2 nuclear immunostaining in a dedifferentiated osteosarcoma.

indel, the tumor sample MAF had to be two times higher than the MAF of the matched control sample.

results

We identified a total of 84 point mutations and 4 deletions related to 82 different genes from our OS samples (Table 1 and supplementary data S1, available at *Annals of Oncology* online). None of them were recurrent mutations but, in three patients, we observed mutations affecting the *TP53* gene (Figure 2). One patient contained a STOP gained mutation at amino acid number 192, and another patient had a nonsynonymous mutation corresponding to amino acid 159 of the TP53 protein followed by two deletions of 3 and 13 bp that leads to a frameshift. A third patient carried a mutation located in the donor splice site of TP53 (corresponding to TP53 amino acid 307). We postulate that this latter mutation leads to the conservation of the intron, resulting in a truncated TP53 protein. Interestingly, in the dedifferentiated OS case, which carried *MDM2* and *CDK4* amplification, no other mutation was detected, suggesting that this tumor subtype is a distinct molecular entity (Figure 3).

discussion

In this study, we carried out whole-exome sequencing of samples from seven OS patients to try to identify new somatic mutations. We compared the mutational profile of six conventional high-grade OS, (comparing tumor and normal tissues from the same patient) and central dedifferentiated OS, known to have a simple genomic profile with *MDM2* amplification. We then examined whether the mutational profile obtained for each patient identified common signaling pathways or biomarkers that might play some role in the pathogenesis of OS. We identified a total of 84 point mutations and 4 deletions related to 82 different genes in OS samples. None of them were recurrent mutations, but in three patients we observed mutations affecting the *TP53* gene (Figure 2). *TP53* has already been described as one of the most mutated genes in OS [8]. Recently, Chen et al. and Perry et al. conducted whole-genome sequencing and whole-exome and RNA sequencing on 20 OS and 59 tumor/normal sample pairs, respectively [6, 7] and identified p53 pathway alterations with a high frequency of mutations mostly in the first intron of the *TP53* gene [8]. The *TP53* gene mutations found in our study were new mutations, not previously described in the dbSNP database. These mutations lead to a truncated form of TP53 with the TP53 transactivation domain

and the entire or a portion of the DNA binding domain but they have lost their oligomerization and C-Terminal regulatory domains (Figure 2). We can postulate that these mutations lead to the degradation of *TP53* mRNA by the nonsense-mediated mRNA decay or that truncated TP53 act as dominant negative mutants on the TP53 wild type as previously described [14]. We also detected a STOP gained mutation (aa829) in the retinoblastoma 1 (*RB1*) gene in one case. This gene is also known to be frequently mutated in OS [1]. In their recent study, Chen et al. investigated recurrent somatic structural variations in pediatric OS and identified 2057 point mutations in 1707 genes [7]. In addition to *TP53* and *RB1*, they observed recurrent somatic alterations of the *ATRX* and *DLG2* genes, with the *ATRX* gene being one of the most frequently mutated genes. In our cohort, however, we did not observe any *ATRX* mutations. This finding may be explained by the size of our series but also by geographical variation since we would expect to detect this alteration in at least two of our cases. Alterations in *CDC27*, a gene controlling the cell cycle, and the *MUC4* and *EI24* genes, have also been recently reported in a single case of OS [10]. We did not find any alteration in these genes in our patients.

However, among the 82 mutated genes described in our study, 15 were also reported by Chen et al., suggesting that these genes are recurrently mutated in OS [7]. Mutations in the *TSC2* gene are our only finding in common with the study by Perry et al. [6] Among the 16 genes described above, some are involved in cell cycle regulation, tumor cell division, transcription and proliferation (*TP53*, *RB1*, *LRRC16B*, *PSD4*, *ADAMS16*, *SALL1*, *EFCAB6*), and others are involved in cytoskeletal integrity, cytoplasmic trafficking and energy metabolism (*SYNE2*, *DNAH6*, *VPS13D*, *DUSP27*). The *CR1* gene found mutated in our study seems to have a predominant role in the immune response and *TSC2* is involved in the PI3K/mTOR pathway [6] making this gene/pathway a potential therapeutic target. However, it should be mentioned that all the point mutations we observed in *CR1*, *LRRC16B*, *SYNE2*, *SALL1*, *PSD4*, *GPRD6A*, *ABCA13*, *RP1L1*, *DUSP27*, *VPS13D*, *EFCAB6* and *TSC2* are new mutations, distinct from those previously reported [6, 7]. These findings emphasize the extreme genomic instability of OS and support the hypothesis that the processes of chromothripsis, defined by tens to hundreds of genomic rearrangements occurring in one-off cellular crisis and which have already been described to have a frequency of 50% in OS [6, 7], is indeed a frequent event in this pathology.

Among the three patients found to have no mutations in the *TP53* and *RB1* genes, one (patient 4) was a dedifferentiated OS.
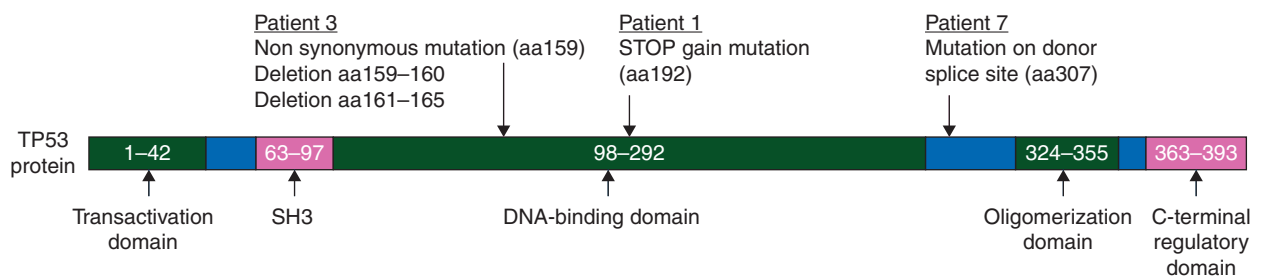

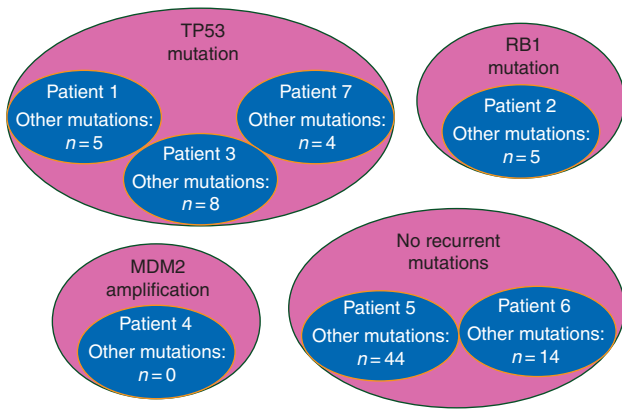**Figure 2.** TP53 mutations observed in three patients.

Figure 3. Mutational spectrum of osteosarcoma isolates distinct subgroups. Note that tumors with either TP53 or RB1 mutations display relative low number of secondary mutations compared with patients with wild-type genes. MDM2 amplification identifies a specific subgroup of tumor devoid of secondary mutations (dedifferentiated osteosarcoma).

Interestingly, even in the dedifferentiated form, no point mutations were found, reinforcing the idea that this subtype of OS with *MDM2* amplification is distinct from the high-grade conventional OS subtype. We also observed that the highest rate of somatic point mutations occurred in cases (patients 5 and 6) that did not contain alterations in the *TP53* and *RB1* genes. These findings suggest that *TP53* mutations and, to some extent, *RB1* mutations are founding events in the process of bone oncogenesis and that, in the absence of these mutations. a higher rate of genetic alteration is required. Of note, patient 5 was the only patient with a poor response to chemotherapy (27% of viable cells) and had the highest number of mutated genes ($n = 45$), suggesting poor response to chemotherapy, and so on; poor prognosis is associated to high level of mutations. We can also hypothesize that patients with *TP 53* gene mutations may have a better response to chemotherapy.

Collectively, in line with previously reported studies our data suggest that OS is an extremely heterogeneous tumor with regard to genetic alterations (Figure 3). Indeed, *TP53* represents a key gene mutated in a significant number of cases. Of particular interest is the wide diversity of *TP53* mutations, all of them leading to inactivation of this tumor suppressor protein and supporting chromothripsis as a critical process in bone oncogenesis. Three main observations arise from our study: (i) whole-exome sequencing has allowed us to identify mutated genes that have not been previously reported in OS; (ii) dedifferentiated OS harboring *MDM2* amplifications do not carry any other mutations, strongly indicating that this subtype represents a clinico-pathological entity with distinct oncogenic mechanisms that requires different therapeutic management (Figure 3); (iii) *TP53* (and *RB1*) inactivation is the strongest oncogenic event in OS development, requiring a limited number of secondary genetic mutations (Figure 3).

These data confirm that the development of targeted therapies for OS will be difficult and that in the future a personalized approach is the most realistic avenue for providing patients with efficient treatment.

disclosure

The authors have declared no conflicts of interest.

references

1. Fletcher CDM, Bridge JA, Hogendoorn PCW, Mertens M. WHO classification of tumour. In: Hogendoorn PCW, Mertens F (eds). WHO Classification of Tumours of Soft Tissue and Bone. Lyon: IARC, 2013.
2. Szymanska J, Mandahl N, Mertens F et al. Ring chromosomes in parosteal osteosarcoma contain sequences from 12q13-15: a combined cytogenetic and comparative genomic hybridization study: genes. Chromosomes Cancer 1996; 16: 31–34.
3. Dujardin F, Binh MBN, Bouvier C et al. MDM2 and CDK4 immunohistochemistry is a valuable tool in the differential diagnosis of low-grade osteosarcomas and other primary fibro-osseous lesions of the bone. Mod Pathol 2011; 24: 624–637.
4. Kansara M, Teng MW, Smyth MJ, Thomas DM. Translational biology of osteosarcoma. Nat Rev Cancer 2014; 14(11): 722–735.
5. Savage SA, Mirabello L, Wang Z et al. Genome-wide association study identifies two susceptibility loci for osteosarcoma. Nat Genet 2013; 45: 799–803.
6. Perry JA, Kiezun A, Tonzi P et al. Complementary genomic approaches highlight the PI3K/mTOR pathway as a common vulnerability in osteosarcoma. Proc Natl Acad Sci USA 2014; 111: E5564–E5573.
7. Chen X, Bahrami A, Pappo A et al. Recurrent somatic structural variations contribute to tumorigenesis in pediatric osteosarcoma. Cell Rep 2014; 7: 104–112.
8. Ribi S, Baumhoer D, Lee K et al. TP53 intron 1 hotspot rearrangements are specific to sporadic osteosarcoma and can cause Li-Fraumeni syndrome. Oncotarget 2015; 6: 7727–7740.
9. Cheung NKV, Zhang J, Lu C et al. Association of age at diagnosis and genetic mutations in patients with neuroblastoma. JAMA 2012; 307: 1062–1071.
10. Reimann E, Kõks S, Ho XD et al. Whole exome sequencing of a single osteosarcoma case—integrative analysis with whole transcriptome RNA-seq data. Hum Genomics 2014; 8: 20.
11. Stephens PJ, Greenman CD, Fu B et al. Massive genomic rearrangement acquired in a single catastrophic event during cancer development. Cell 2011; 144: 27–40.
12. Meyerson M, Pellman D. Cancer genomes evolve by pulverizing single chromosomes. Cell. 2011;144: 9–10.
13. Cordonnier T, Langonné A, Sohier J et al. Consistent osteoblastic differentiation of human mesenchymal stem cells with bone morphogenetic protein 4 and low serum. Tissue Eng Part C Methods 2011; 17: 249–259.
14. de Vries A, Flores ER, Miranda B et al. Targeted point mutations of p53 lead to dominant-negative inhibition of wild-type p53 function. Proc Natl Acad Sci USA 2002; 99: 2948–2953.